



Biomedical Imaging

By

James E. Bruckart

Aircrew Protection Division

April 1994

Approved for public release; distribution unlimited.

**United States Army Aeromedical Research Laboratory
Fort Rucker, Alabama 36362-0577**

Notice

Qualified requesters

Qualified requesters may obtain copies from the Defense Technical Information Center (DTIC), Cameron Station, Alexandria, Virginia 22314. Orders will be expedited if placed through the librarian or other person designated to request documents from DTIC.

Change of address

Organizations receiving reports from the U.S. Army Aeromedical Research Laboratory on automatic mailing lists should confirm correct address when corresponding about laboratory reports.

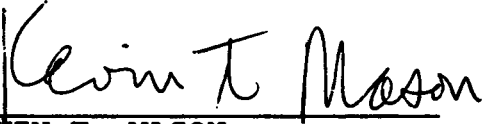
Disposition

Destroy this document when it is no longer needed. Do not return it to the originator.

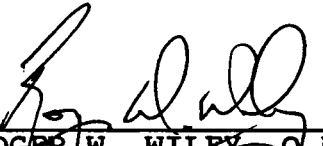
Disclaimer


The views, opinions, and/or findings contained in this report are those of the author(s) and should not be construed as an official Department of the Army position, policy, or decision, unless so designated by other official documentation. Citation of trade names in this report does not constitute an official Department of the Army endorsement or approval of the use of such commercial items.

Reviewed:


KEVIN T. MASON
LTC, MC, MFS
Director, Aircrew Protection
Division

Released for publication:


ROGER W. WILEY, O.D., Ph.D.
Chairman, Scientific
Review Committee


DAVID H. KARNEY
Colonel, MC, SFS
Commanding

REPORT DOCUMENTATION PAGE				Form Approved OMB No. 0704-0188	
1a. REPORT SECURITY CLASSIFICATION Unclassified			1b. RESTRICTIVE MARKINGS		
2a. SECURITY CLASSIFICATION AUTHORITY			3. DISTRIBUTION/AVAILABILITY OF REPORT Approved for public release, distribution unlimited		
2b. DECLASSIFICATION/DOWNGRADING SCHEDULE					
4. PERFORMING ORGANIZATION REPORT NUMBER(S) USAARL Report No. 94-21			5. MONITORING ORGANIZATION REPORT NUMBER(S)		
6a. NAME OF PERFORMING ORGANIZATION U.S. Army Aeromedical Research Laboratory		6b. OFFICE SYMBOL (if applicable) SGRD-UAD-IE	7a. NAME OF MONITORING ORGANIZATION U.S. Army Medical Research, Development, Acquisition and Logistics Command		
6c. ADDRESS (City, State, and ZIP Code) P.O. Box 620577 Fort Rucker, AL 36362-0577			7b. ADDRESS (City, State, and ZIP Code) Fort Detrick Frederick, MD 21702-5012		
8a. NAME OF FUNDING/SPONSORING ORGANIZATION		8b. OFFICE SYMBOL (if applicable)	9. PROCUREMENT INSTRUMENT IDENTIFICATION NUMBER		
8c. ADDRESS (City, State, and ZIP Code)					
			10. SOURCE OF FUNDING NUMBERS		
			PROGRAM ELEMENT NO. 62787A	PROJECT NO. 30162787A878	TASK NO. EA
11. TITLE (Include Security Classification) Biomedical Imaging					
12. PERSONAL AUTHOR(S) James E. Bruckart					
13a. TYPE OF REPORT		13b. TIME COVERED FROM _____ TO _____		14. DATE OF REPORT (Year, Month, Day) 1994 April	
15. PAGE COUNT 19					
16. SUPPLEMENTARY NOTATION					
17. COSATI CODES			18. SUBJECT TERMS (Continue on reverse if necessary and identify by block number) Biomedical imaging, anthropometry, computer imaging		
FIELD	GROUP	SUB-GROUP			
05	02				
05	09				
19. ABSTRACT (Continue on reverse if necessary and identify by block number) This paper has been prepared for submission to the Advisory Group for Aerospace Research and Development (AGARD) Working Group 20 as a chapter on three-dimensional image collection for a report on 3D anthropometry. The principal 3D anthropometry data acquisition task, imaging the human body, presents technical barriers. The ultimate choice of an imaging technique depends on the specific details of an object that require reproduction and the precision required from the task. This report details the technologies in surface and subsurface imaging systems for research and commercial applications.					
20. DISTRIBUTION/AVAILABILITY OF ABSTRACT <input checked="" type="checkbox"/> UNCLASSIFIED/UNLIMITED <input type="checkbox"/> SAME AS RPT. <input type="checkbox"/> DTIC USERS			21. ABSTRACT SECURITY CLASSIFICATION Unclassified		
22a. NAME OF RESPONSIBLE INDIVIDUAL Chief, Science Support Center			22b. TELEPHONE (Include Area Code) 205-255-6907		22c. OFFICE SYMBOL SGRD-UAX-SI

Foreword

This paper has been prepared for submission to the Advisory Group for Aerospace Research and Development (AGARD) Working Group 20. It is intended as a chapter on three-dimensional image collection for an upcoming report on 3D anthropometry to be published by the working group.

=====

This page intentionally left blank.

=====

Biomedical Imaging

**James E. Bruckart, M.D.
U.S. Army Aeromedical Research Laboratory**

Introduction

Geometric information about biomedical objects can be collected using various physical methods or modalities including optical, x-ray, acoustic, radioactivity, and nuclear magnetic resonance properties. The two most common are direct observation and photography. These have been used for traditional anthropometry and medical imaging, but some tasks require precise measurements or internal details not easily determined by observation.

Use of an image data collection tool offers several potential advantages in inspecting objects. First, some imaging methods provide internal structural details that may not be discerned from external examination. Second, imaging sensors can provide precise and complete geometric data from visible surfaces. These data can be used for measurement of biomedical objects with irregular shapes and provide the basis for evaluating volumetric properties. Third, images from several sources (multimodality) can be fused to form composite images. Finally, the coordinate data may be useful in generating physical replicas.

The imaging technology chosen for a specific task depends on the properties of the object that are being evaluated and the precision requirements. For example, a laser scan that produces a precise surface image of a human head will not provide the internal anatomic details that are available with x-ray computerized tomography (CT scan). Likewise, the clinical CT scan will not provide the microscopic surface details required to produce an image of a fingerprint.

Each unique imaging modality has inherent strengths and deficiencies. Optical methods are superior for distant objects while magnetic resonance imaging provides very accurate information if the object is near the imaging system. The principal 3D anthropometry data acquisition task, imaging the human body, presents several technical barriers. For example, should the imaging system provide complete coverage, such as details on the sole of the foot? Is the same level of detail required for the face, extremities, and abdomen, or should they be imaged separately? The ultimate choice of an imaging technique depends on the specific details of an object that require reproduction and the precision required from the task. Strategies for imaging and archiving the human body will be discussed in other sections of this report. This chapter details the technologies in surface and subsurface imaging systems for research and commercial applications.

Traditional anthropometry

The single constant in artistic and industrial efforts is the human body as a central focus. Whether the project is to create a new hand tool, build an aircraft, or design a new garment, first the human body must be measured to ensure the finished product will serve its intended purpose. Anthropometry is the practice of measuring the human body.

To assist designers and engineers, anthropometry is collected for body segments that come in contact with a planned device. Most often the anthropometric measures are linear distances between identifiable landmarks on the body, but body weight or other measures may be included. (1) An anthropometry survey involves the collection of measurements for a population group. The results of an anthropometry survey generally are reported as summary statistical measures, such as mean and standard deviation, for each body segment. Every survey is unique in terms of the population studied and the specific body segments that are measured. To improve comparability, most anthropometry surveys also include specific details on the age, sex, and ethnic groups of the individuals in the study population. A summary of anthropometric surveys of 61 military and civilian populations are described in NASA Reference Publication 1024. (2)

Several important decisions are required when designing and implementing an anthropometry survey. First, the survey subjects should represent the population that is being evaluated. For example, measures for use in designing military aircraft should be obtained from a survey of military pilots. Second, the body segments to be measured and the measurement position should reproduce the functional position for using the device. Of course, completing an anthropometry survey for each design task is impractical. Most anthropometry surveys collect measures in several postures to provide a set of measures that can be used in various design tasks. Finally, the landmarks on the body and measurement methods should be clearly defined. For example, the method to measure "stature" is defined for the 1988 anthropometric survey of U.S. Army Personnel as:

The vertical distance from a standing surface to the top of the head is measured with an anthropometer. The subject stands erect with the head in the Frankfort plane. The heels are together with the weight distributed equally on both feet. The shoulders and upper extremities are relaxed. The measurement is taken at the maximum point of quiet respiration. (3)

In traditional anthropometry, mechanical aids such as an anthropometer, calipers (sliding or spreading), tape measures, and scales assist observers in measuring body segments. This method provides a linear measure of a body segment, but sacrifices the three-dimensional relation of adjacent body structures. Modern biomedical imaging tools provide the means to obtain accurate three-dimension images.

Imaging Systems

The modalities used to image the surface and internal details of objects have been developed to meet the requirements of different medical and manufacturing applications. These applications include medical imaging of the human body for description and diagnosis, computer modeling of objects for computer-assisted design and manufacture, cartography, and robotic vision. As a result, there are various data collection systems and data formats used in each imaging method.

The data collection methods generally are separated into those whose principal application requires the description of surface details and those that require internal (volume) details. Most of the surface imaging methods use nonpenetrating energy, such as laser light, to provide range information on surface morphology. Volumetric imaging systems use penetrating energy, such as electromagnetic radiation or sound waves, to gather information on internal structures. However, some overlap of methods is evident. For example, skin surface details may be derived from x-ray CT scan data.

A range-imaging sensor is a combination of hardware and software capable of producing distance measurements from a known reference coordinate system to points on an object. The point positions (x,y,z) are captured within a specified accuracy or error tolerance. Four basic types of range sensors are distinguished by their viewing constraints, scanning mechanisms, and object motion. A *point sensor* measures the distance to a single visible surface point from a single viewpoint along a light line or ray. A point sensor can create an image of an object if the object is moved relative to the sensor or the sensor moves relative to the object. A *line* or *circle sensor* measures the distance to visible surface points that lie in a single plane or cone that contains the viewpoint. A *field-of-view sensor* measures the distance to many visible surface points that lie within a given field-of-view relative to a single viewpoint. A *multiple view sensor system* locates surface points relative to several viewpoints.

Surface scanning methods

Jarvis (4) and Besl (5), among others, have completed broad surveys of range-imaging methods. These surveys include details on sensing methods, available sensors, and representative performance specifications for these devices. These reviews were used to compile information on the image sensors and technologies available for surface scanners.

Optical sensors use a variety of methods to collect three-dimensional coordinate data from object surfaces. These methods are segregated to those that observe on the axis of illumination and those that observe off the axis.

On-axis observations

Several species of mammals, including bats and porpoises, use sound waves to determine their distance from objects (6, 7). In much the same way, the time required for a radio wave to reflect from a distant object to a receiver is used to determine the distance from the object to the receiver. These systems make use of *time-of-flight* to determine the distance from the object to the receiver.

Several time-of-flight imaging laser radars have been developed. For example, Lewis and Johnston developed an imaging laser radar for the Mars rover that compiled 64 X 64 range images in 40 seconds (8). Several airborne surveying systems are available commercially. One system measures water depths to 40 m with an accuracy of 0.3 m (9) while another provides up to 2000 readings per second with an accuracy of 1 cm at a typical 10 to 500 m range (10).

A variation on the time-of-flight imaging radar uses an amplitude modulated (AM) laser. The range is computed by detecting the phase shift between the transmitted and received signal. Amplitude modulated lasers have been built for research programs and several are available commercially (11, 12). The Perkin-Elmer airborne laser radar scans 2790 pixels per scan line in 2 ms. The forward motion of the scan line is provided by the aircraft's motion (13).

Another method of image ranging can be provided by varying the optical frequency of the laser, termed frequency modulation (FM). The reflected return signal is mixed with the reference signal at the detector. The beat frequency that is created depends on the range of the object (14). This detection process is termed FM coherent heterodyne detection. Two commercially available FM imaging laser radars are reported by Hersman et al. (15).

The surface characteristics and range of an object also can be determined by focusing the image of the object (16, 17). Rioux and Blais (18) developed two techniques using lens focusing properties for ranging. The first uses a grid of point sources projected onto the scene. The range to each point is determined by the radius of the blur in the focal plane of the camera. In the second, a multistriple illuminator shines on the scene. If the stripe is not in focus, the camera sees split lines. The distance between lines is proportional to the distance to the surface. Paradoxically, the autofocus mechanism in cameras frequently use other methods of ranging. For example, the Canon "Sure-Shot" autofocus mechanism is an active triangulation system using a frequency modulated infrared beam (19).

Off-axis observations

Triangulation uses the law of sines to measure the range to a remote object. An example of an active triangulation system is shown in Figure 1 (adapted from reference 5).

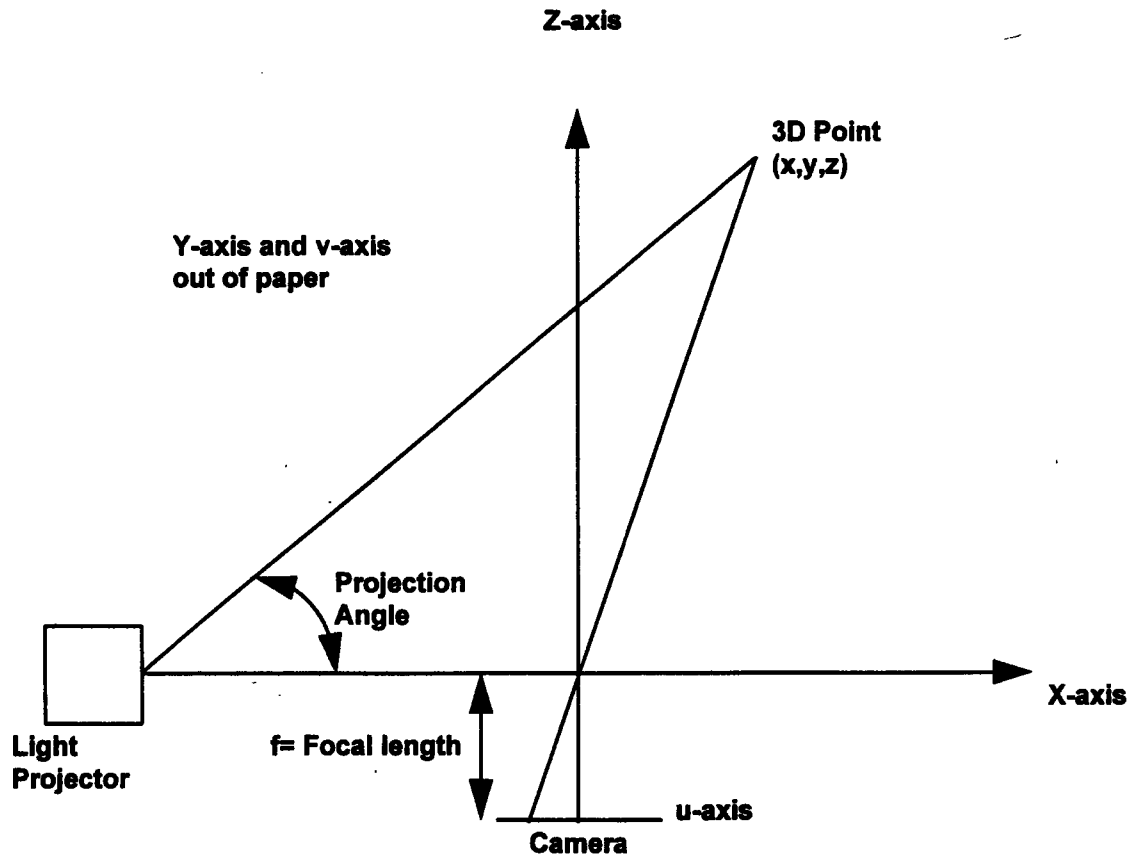


Figure 1. Camera-centered active triangulation system geometry.

A camera is located with the center of the lens at the origin (0,0,0). A light projector, placed a known distance (b) from the camera, sends out a beam or plane of light at a variable angle relative to the x-axis baseline. The 3D point (x,y,z) is projected to an image at the pixel (u,v) in the camera with focal length f . The measured quantities (u,v,f) are used to compute the (x,y,z) coordinates.

Commonly, it is held that a large distance between the light source and the detector is required for accurate ranging. However, the ability of a ranging device is limited instead by the accuracy available to measure the angle and the (u,v) pixel resolution.

The structured light that is projected onto the object can be focused to a point or a line. Point scanning systems will project the light in a horizontal and vertical range to create a composite image of the scene. Commercially available spot scanning systems project white or laser light to detect range information (20-23).

Passing a laser through a cylindrical lens creates a line of light. The light stripe changes shape as it traverses the surface of a three-dimensional object. Changes in line

shape are detected for successive images to determine the three-dimensional shape of an object. Commercially available light stripe scanners are used for industrial applications, scanning human heads, and robot vision systems (24-31).

A moire pattern is an interference pattern created when two gratings with regularly spaced patterns are superimposed on one another (23, 33). In moire range-imaging sensors, surface depth is recovered from the phase difference obtained after the signal is filtered with a low-pass filter. Moire range-imaging is most useful for measuring the relative distance to surface points on a smooth surface. Commercially available moire scanners use projected light, shadow, or framing techniques (34-37).

Holographic interferometers use coherent light from laser sources to produce interference patterns due to the optical frequency phase differences in different optical paths. Surface depth information is recovered from the phase difference term. Just as in moire range imaging, the measured surfaces must be smooth and flat. This technology is useful in commercial applications to visualize stress, thermal strain, pressure effects, erosion, microscopic cracks, fluid flow, and other physical effects in nondestructive testing (38-41).

Summary

The key factors in the performance of a range-imaging system are the depth of field, range accuracy, pixel rate, range resolution, image size, angular field-of-view, standoff distance, and frame rate. A series of images produced with a range sensor using a 1.8 square meter sampling array are shown in Figure 2. The surface sampling parameters, including the sampling distance along each axis, total area scanned, number of pixels, and file size, are shown in Table 1. The addition of intensity (I) or color (RGB) information increases the size of the data file as indicated.

Table 1. Surface sampling parameters for a 1.8 m² image sensor*.

X(mm)	Y(mm)	Z(mm)	Area (mm ²)	Total pixels	File size (Mbytes)		
					3D	3D+I	3D+RGB
0.05	0.05	0.005	1/400	7.2x10 ⁸	1440	2160	3600
0.9	0.9	0.040	0.81	2.2x10 ⁶	4.4	6.6	22
1	1	0.1	1	1.8x10 ⁶	3.6	5.4	18
2	4	0.4	8	2.2x10 ⁵	0.45	0.67	1.1
5	5	1	25	7.2x10 ⁴	0.14	0.23	0.36

*from National Research Council Canada.

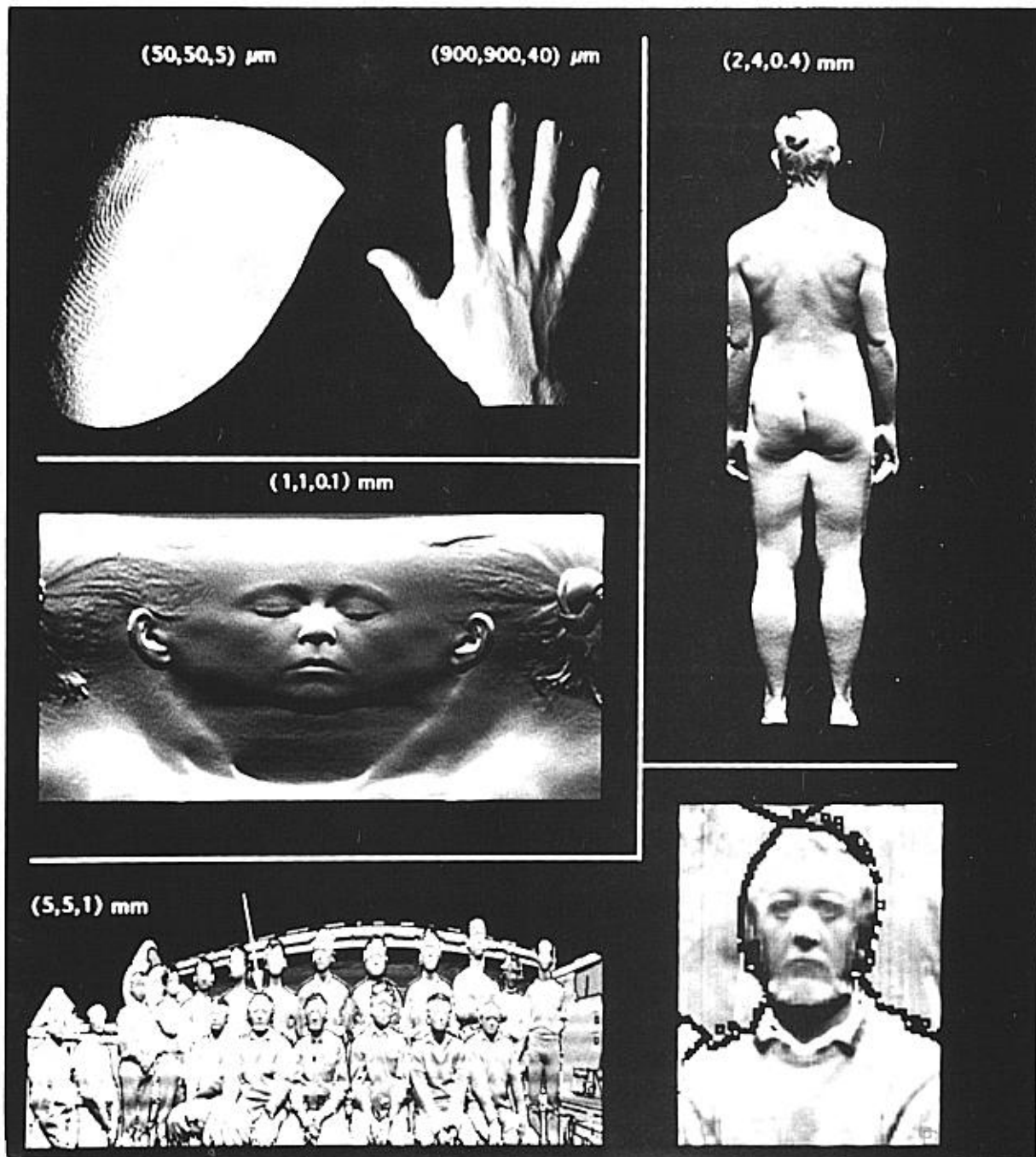


Figure 2. Representative images from a 1.8 m² image sensor.

Imaging laser radars are capable of accuracies from $50\ \mu$ to 5 m over depths of field 250 to 25,000 times larger. Usually they are expensive with commercially available units starting at around \$100,000. Triangulation sensors are capable of range accuracies of about $1\ \mu$ over depths of field of 250 to 60,000 times larger. Simple systems start at \$1000 and range to several hundred thousand dollars. Moire systems provide the same accuracy as triangulation sensors, but only if the surface constraints are met. Fast computer hardware is needed for the computations which will total more than \$50,000 for a reasonably fast system. Holographic interferometer systems have the advantage of measuring with accuracies of less than a half a nanometer, but surface slope and smoothness constraints apply. Active focusing systems hold promise as inexpensive range sensors, but high precision systems are not likely (5).

Tactile methods still dominate most applications where the exact shape of a prototype object must be duplicated. However, coordinate measuring machines inherently are slow and expensive. Optical noncontact imaging methods will produce a cost savings if they are fast, accurate, reliable, and easy to use (5).

Volumetric imaging methods

Volumetric imaging of the human body has leapt forward with demands for improved images as diagnostic tools in medicine. Most diagnostic imaging is done in the radiology department and is segregated into five categories: ultrasound imaging, x-ray computed tomography, magnetic resonance imaging, nuclear scintigraphy (including PET and SPECT), and conventional projection radiography. These imaging modalities provide details on internal structures and usually are viewed with transparent film hard copy on a fluorescent back light box in a two-dimensional format. However, advances in computer processing of volume data and enhanced tools to present three-dimensional scenes guarantee an increased demand for three-dimensional rendering of these images (42-43).

Ultrasound imaging

Vascular disease is a very common human affliction. While x-ray angiography, using radiopaque contrast, remains the mainstay in diagnosis of cardiovascular abnormalities, ultrasonic imaging of vascular structures provides important information on anatomic structures and vascular flow. Ultrasound depends on the differential transmission, absorption, scattering and reflection of sound waves from constituent biological materials to provide information on internal structures and blood flow (42, 44). The technique is best when imaging soft tissue object surfaces or thin-shelled volumes, and is poorly suited to access centrally located areas (43). Combining gray-scale ultrasound imaging of internal structures and Doppler for blood flow results in duplex Doppler with simultaneous imaging

of anatomic structures and circulatory physiology. In addition, color displays enhance duplex Doppler by providing color-coded images of blood flow (42).

The principal uses for ultrasound imaging in medicine are for the diagnosis of carotid bifurcation disease (45), evaluation of valvular disease and shunts (42), thyroid, testis, and abdominal diagnosis, endourology, and imaging the developing fetus. However, the relatively low cost and noninvasive nature of the test make it useful in evaluating tissue layering and masses anywhere in the body. This is a noninvasive technology which does not expose the subject to ionizing radiation (46).

There are several practical limitations in the use of ultrasound for three-dimensional reconstruction of the human form. First, most ultrasound studies do not use fixed reference points on the body and data acquisition is limited to two dimensions. Interpolation of two-dimensional images to three dimensions is simplified in CT and MRI scans because successive images are parallel and equidistant. This is usually not the case for ultrasound images (43). Second, the quality and form of the images depend on the skill of the operator. Third, the ultrasound probe requires direct contact with the skin. Finally, ultrasound images of structures near the skin surface are readily visualized, but osseous structures or structures within the chest cavity are not. Many soft tissue organs visualized by ultrasound are continuously deformable and consistent 3D data cannot be acquired easily.

High resolution computed tomography

In a conventional radiograph, transmitted x-rays form a composite image of the internal structure of the body. The amount of radiation that passes through the body is inversely proportional to the density (radiopacity or attenuation and scatter) of the tissues. Plain radiographs provide excellent spatial resolution, but soft tissue discrimination is relatively poor, and overlapping structures can obscure details (47).

X-ray computed tomography was introduced in the 1970s and the 1979 Nobel Prize for Medicine was awarded to Cormack and Hounsfield for this development (48, 49). In computer-assisted tomographic scanners, multiple radiosensitive detectors view a moving x-ray source. The computer reconstructs the data into slice images. From early units with a low resolution and 1.5 cm slice thickness have emerged current high resolution CT scanners. With the high resolution technique, a 512 x 512 reconstruction and display matrix can be concentrated in a small region of the skull and slice thickness can be reduced to 1 or 2 millimeters (47). High resolution CT is used widely in clinical medicine, particularly when evaluating masses in the head, chest, and abdomen (42). Spiral CT scanning recently was introduced to acquire volumetric data sets.

CT images provide excellent bony details and soft tissue features, but to gain a three-dimensional appreciation of an object, the observer must mentally integrate numerous

sequential two-dimensional images. This interpolation is facilitated somewhat when the two-dimensional images are parallel and equidistant. Computer software has been developed to allow reformation of the CT data to reconstruct a model of the internal details. The reconstruction of axial images often are displayed in rotational projections of three-dimensional structures (46, 47).

Three-dimensional reconstruction algorithms have been described (50) and usually adopt one of two strategies:

1. Surface: Two-dimensional contours are extracted from each image. The contours are stacked and geometric interpolation is used to produce the three-dimensional object surface (51, 52).
2. Volume: A three-dimensional array of CT numbers is created from the series of tomograms. Each pixel generates a volume element or "voxel" reflecting the thickness of each tomogram slice (53).

There are two principal methods for displaying three-dimensional information generated in this manner. These are the indirect projection mode and direct three-dimensional mode. In the indirect approach, the three-dimensional object is projected onto an image plane from a given point-of-view. Depth is added to the scene by brightness coding, simulated light sources, texturing, or continuous rotation of the object. Direct three-dimensional representation requires special hardware such as varifocal mirrors (54) or multiplex holography (55). The use of direct 3D is infrequent in practice, owing to the physical limitations of the viewing apparatus.

Since CT and MR scanners are computer based, it is possible to perform the 3D imaging on the scanner and avoid the cost of additional hardware. Nevertheless, a stand-alone three-dimensional imaging system may be preferred to avoid interfering with the usage of the scanner. The length of time required to generate a three-dimensional image from the scanner data may be only a few seconds for a specially designed hardware and software system to a few minutes for on-the-scanner software. Of particular concern in this case is whether the three-dimensional image is required for direct interaction or for later review (56).

Magnetic resonance imaging

More recent than computerized tomography, magnetic resonance (MR) makes use of proton distribution within biological tissues to produce images of internal structures. The relatively high density of mobile H^+ ions in body tissues allow detectable nuclear magnetic resonance signals to be induced. To measure the MR signal emitted from nuclei, such as hydrogen, sodium-23, phosphorus-31, and carbon-13, an applied magnetic field and second

on-and-off magnetic field is used in synchrony with the frequency of the nucleon measured. The detected MR signal is radio frequency (RF) pulses. The location of the MR signal in the electromagnetic spectrum is shown in Figure 3. RF stimulation adds energy to the system and causes protons to move to a higher energy state. Dissipation of this energy and return of the protons to the lower energy state is known as T1 relaxation. T2 relaxation results from dephasing of spins as an effect of local magnetic field inhomogeneities due to randomly varying intrinsic magnetic fields created by adjacent nuclei. The MR contrast effects, including T1 or T2 relaxation times, flow, spin density, chemical shift, magnetic susceptibility, or other factors, manifest themselves as signals detected by the RF coil (42, 57).

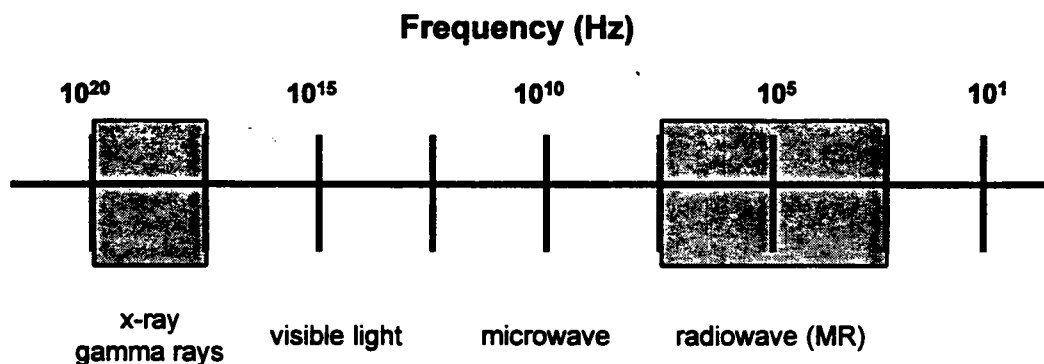


Figure 3. Location of the MR signals in the electromagnetic spectrum.

After application of excitatory RF pulses, the amplitude of the MR signal decays to zero. This causes detectable signal losses in the sample due to T1 and T2 relaxation effects.

The relaxation rates depend on the composition and local environment of the protons in the sample. In other words, the relaxation effects indicate the chemical structures in the local environment. Image contrast is based on the difference in signal intensity between areas of different structure or composition. Superior soft tissue contrast resolution is one of the greatest advantages of MR imaging over computed tomography (58-59)

Magnetic resonance imaging's strengths include its lack of ionizing radiation and its sensitivity to flow. This is particularly useful for patients requiring multiple examinations, pediatric patients, and pregnant patients. In computed tomography, the scan plane is defined by the x-ray tube-detector axis. In MR imaging, the scan plane is defined by the selection of RF frequencies and magnetic field gradients. This makes multiplanar studies possible. Magnetic resonance is weak in the areas of calcium sensitivity, acute hemorrhage, and when

pacemakers or other electronic devices interfere (42). Since MR imaging is recent, its potential has not been fully exploited and its comparative advantages for three-dimensional object reconstruction remain to be firmly established (43).

Other imaging methods

After World War II, biomedical science was revolutionized by the introduction of carbon-14 and tritium as radioactive tracers. While these agents have been valuable in laboratory research, their beta emissions could not penetrate the body and be detected by imaging devices. More recently, nuclear magnetic resonance spectroscopy (MRS), single photon emission computed tomography (SPECT), and positron emission tomography (PET) make it possible to examine the structure of the living body *in situ* through its chemical processes. Nuclear magnetic resonance spectra of molecules containing naturally occurring phosphorus-31 or administered fluorine-19 or carbon-13 make it possible to measure molecular concentrations of important compounds, such as ATP, inorganic phosphorous, and chemical reaction rates in different organs and tissues. PET is based on the use of carbon-11 or fluorine-18 and SPECT is based on iodine-123, technetium-99, and indium-111. These nuclides emit photons that can be detected and imaged. Abnormal tissue can be defined in terms of variation from normal regional chemistry (60).

Summary

A number of imaging methods have evolved to provide diagnostic tools for clinical medicine. High resolution CT imaging is the most mature of these new three-dimensional imaging methods and currently has the greatest application in producing composite images. However, comparable evolution is expected in MR and newer imaging methods that will provide data for three-dimensional reconstruction of internal structure.

Conclusions

A number of methods currently are available to collect three-dimensional surface and subsurface detail on three-dimensional objects. Several techniques for surface imaging provide very accurate measurements of the human form. High resolution computer tomographic images already are reconstructed to permit three-dimensional representation of internal structures. Other medical imaging methods of internal structures will allow similar capabilities.

Significant problems remain in producing a composite image with data collected from several sources. Standard body reference points and data formats are needed to allow direct comparison of this data. In addition, enhanced software tools and innovative displays will improve the useability of three-dimensional image data.

References

1. Shephard, R. J.
Body composition in biological anthropology. Cambridge University Press.
Cambridge. 1991.
2. Webb Associates.
Volume II: A handbook of anthropometric data. National Aeronautics and Space
Administration. Houston, TX. 1978. NASA RP-1024.
3. Gordon, C. C., Churchill, T., Clauser, C. E., Bradtmiller, B., McConville, J. T.,
Tebbetts, I., and Walker, R. A.
1988 Anthropometric survey of U.S. Army personnel: Summary statistics interim
report. U.S. Army Natick Research, Development and Engineering Center. Natick,
MA. 1989. Technical Report NATICK/TR-89/027.
4. Jarvis, R. A.
A perspective on range finding techniques for computer vision. IEEE Transactions
Pattern Analysis Machine Intelligence PAMI-5, 1983: 122-139.
5. Besl, P.J.
Active Optical Range Imaging Sensors. Machine Vision and Applications. 1, 1988:
127-152.
6. Griffin, D.R.
Listening in the dark: The acoustic orientation of bats and men. New Haven, CT.
Yale University Press, 1958.
7. Kellogg, W.N.
Porpoises and sonar. Chicago, IL. University of Chicago Press, 1961.
8. Lewis R.A., and Johnston, A. R.
A scanning laser range finder for a robotic vehicle. Proceedings 5th International
Joint Conference on Artificial Intelligence, 1977: 762-768
9. Banic, J., Sizgoric, S., and O'Neill, R.
Airborne scanning lidar bathymeter measures water depth. Laser Focus/Electro-
Optics, 1987: 48-52.
10. Optec Systems Corporation
Model 501SA/501SB Laser Rangefinder product information. Toronto, Canada.
1991.

11. Binger, N., and Harris, S. J.
Applications of laser radar technology. *Sensors*, 4(4), 1987: 42-44.
12. Svetkoff, D. J.
Towards a high resolution, video rate, 3D sensor for machine vision. *Proceedings SPIE conference on Optics, Illumination, and Image Sensing for Machine Vision*, 728, (1986): 216-226.
13. Keyes, R. J.
Heterodyne and nonheterodyne laser transceivers. *Review of Scientific Instrumentation*. 57(4), 1986: 519-528.
14. Skolnick, M. I.
Introduction to radar systems. New York. McGraw-Hill. 1962.
15. Hersman, M., Goodwin, F., Kenyon, S., and Slotwinski, A.
Coherent laser radar application to 3D vision and meteorology. *Proceedings Vision '87 Conference*, 3-1-3-12. 1987.
16. Jarvis, R. A.
Focus optimization criteria for computer image processing. *Microscope*. 24(2), 1976: 163-180.
17. Krotkov, E., and Martin, J. P.
Range from focus. *Proceedings IEEE International Conference on Robotics and Automation*. IEEE-CS, 1986: 1093-1098.
18. Rioux, M., and Blais, F.
Compact 3-D camera for robotic applications. *Journal of Optical Society of America*. 3(9), 1986: 1518-1521.
19. Jarvis, R. A.
Computer vision and robotics laboratory. *IEEE Computer*. 15(6), 1982: 505-512.
20. Vannier, M. W., Pilgram, T., Bhatia, G., Brunsten, B., and Commean, P.
Facial surface scanner. *IEEE Computer Graphics and Applications*. Washington, D.C., 1991: 72-80.
21. Cyberoptics.
Product information. Minneapolis, MN. 1987.

22. Gottwald, R. and Berner, W.,
The new Kern system for positioning and automated coordinate evaluation: advanced technology for automated 3D coordinate determination. Product information. Brewster, N.Y. 1987.
23. Selcom.
Optocator product information. Valdese, NC. 1987.
24. Schmitt, F., Barsky, B., Du, W.
An adaptive subdivision method for surface-fitting from sampled data. Computer Graphics. 20(4), 1986: 179-188.
25. Baribeau, R., Rioux, M., Godin, G.
Color reflectance modeling using a polychromatic laser range sensor. Transactions on Pattern Analysis and Machine Intelligence. IEEE. Washington, DC. 1993.
26. Cyberware.
Product information. Monterey, CA. 1993.
27. Robotic Vision Systems, Inc.
Product information. Hauppauge, NY. 1987.
28. Rioux, M., Blais, F., Beraldin, J.-A., and Boulanger, P.
Range imaging sensors development at NRC laboratories. Proceedings of the Workshop on Interpretation of 3D Scenes. IEEE. Washington, DC. 1989: 154-160.
29. Nahas, M., Huitric, H., Rioux, M., and Domey, J.
Registered 3D-texture imaging. In Computer Animation '90, Magnenat-Thalmann and Thalmann (eds), Springer-Verlag, 1990: 81-90.
30. Blais, F., Rioux, M., Beraldin, J.-A.
Practical considerations for a design of a high precision 3-D laser scanner system. In Proceedings: Optomechanical and Electro-Optical Design of Industrial Systems. SPIE Vol. 959. Washington, DC. 1988: 225-246.
31. Beraldin, J.-A., Rioux, M., Blais, F., Godin, G., and Barbeau, R.
Model-based calibration of a range camera. In Proceedings: International Conference on Pattern Recognition. IEEE. Washington, D.C. 1992: 163-167.
32. Sciammarella, C. A.
The moire method-A review. Exp Mech. 22, 1982: 418-433.

33. Pirodda, L.
Shadow and projection moire techniques for absolute and relative mapping of surface shapes. *Optical Engineering*. 21, 1982: 640
34. Electro-Optical Information Systems.
Product information. Santa Monica, CA. 1987.
35. Cline, H.E., Lorenson, W. E., and Holik, A.S.
Automated moire contouring. *Applied Optics*. 23(10), 1984: 1454-1459.
36. Halioua, M., Krishnamurthy, R.S., Liu, H., and Chiang, F. P.
Projection moire with moving gratings for automated 3D topography. *Applied Optics*. 22(6), 1983: 850-855.
37. Reid, G. T.
Automatic fringe pattern analysis: A review. *Optics and lasers in Engineering*. 7, 1986: 37-68.
38. Tozer, B. A., Glanville, R., Gordon, A. L., Little, M. J., Webster, J. M., and Wright, D. G.
Holography applied to inspection and measurement in an industrial environment. *Optical Engineering*. 24(5), 1985: 746-753.
39. Mader, D. L.
Holographic interferometry of pipes: precision interpretation by least squares fitting. *Applied Optics*. 24(22), 1985: 3784-3790.
40. Wuerker, R. F., and Hill, D. A.
Holographic microscopy. *Optical Engineering*. 24(3), 1985: 480-484.
41. Church, E. L., Vorburger, T. V., and Wyant, J. C.
Direct comparison of mechanical and optical measurements of the finish of precision machined optical surfaces. *Optical Engineering*. 24(3), 1985: 388-395.
42. Huang, H. K., Aberle, D. R., Lufkin, R., Grant, E. G., Hanafee, W. N., and Kangerloo, H.
Advances in medical imaging. *Annals of Internal Medicine*. 112(3), 1990: 203-220.
43. deGuise, J. A., and Roberge, F. A.
Using structural and visual information in physiological systems modeling. *Medical Progress through Technology*. 15, 1989: 217-225.

44. Feigenbaum, H.
Echocardiography, 4th ed. Philadelphia. Lea & Febiger. 1986.
45. Jacobs, N. M., Grant, E. G., Schellinger, D., Byrd, M. C., Richardson, J. D., and Cohan, S. L.
Duplex carotid sonography: criteria for stenosis, accuracy, and pitfalls. Radiology. 154, 1985: 385-391.
46. Marsh, J. L., Vannier, M. W., Gado, M., and Stevens, W. G.
In vivo delineation of facial fractures: The application of advanced medical imaging technology. Annals of Plastic Surgery. 17(5), 1986: 364-376.
47. Vannier, M. W., and Marsh, J. L.
Craniofacial Imaging. Lippincott's Reviews: Radiology. 1(2), 1992: 193-209.
48. Cormack, A. M.
Representation of a function by its line integrals with some radiological applications. J Appl Phys. 34, 1963: 2722-2727.
49. Hounsfield, G. N.
Computerized transverse axial scanning tomography. Part I: Description of the system. Br J Radiol. 46, 1973: 1016-1022.
50. Robb, R. A.
Three-dimensional biomedical imaging, CRC Press, Florida. 1985.
51. Batnizky, S., Price, H. L., Cook, P. N., Cook, L. T., and Dwyer, S. J.
Three-dimensional computer reconstruction from surface contours for CT head examinations. J of Comput Assist Tomography. 5, 1981: 60-67.
52. Christiansen, H. N., and Sederberg, T. W.
Conversion of complex contour definitions into polygonal element mosaics. Comput Graphics. 12, 1978: 187-192.
53. Herman, G. T., and Liu, H. K.
Display of three-dimensional information in computed tomography. J of Comput Assist Tomography. 1, 1977: 155-160.
54. Harris, L. D., Camp, J. J., Ritman, E. L., and Robb, R. A.
Three-dimensional display and analysis of tomographic volume images utilizing a varifocal mirror. IEEE Trans Med Images. MI-5, 1986: 67-72.

55. Fujioka, M.
Holography of 3D surface reconstructed CT images. J of Comput Assist Tomography. 12, 1988: 175-178.
56. Herman, G. T.
A survey of 3D medical imaging technologies. IEEE Engineering in Medicine and Biology. 1990: 15-17.
57. Smith, R. C., and McCarthy, S.
Physics of magnetic resonance. J Repro Med. 37(1), 1992: 19-26.
58. Edelstein, W. A., Bottomley, P. A., Hart, H. R., and Smith, L. S.
Signal, noise and contrast in nuclear magnetic resonance (NMR) imaging. J Comp Assist Tomography. 7, 1983: 391-401.
59. Hendrick, R. E., Nelson, T. R., and Hendee, W. R.
Optimizing tissue contrast in magnetic resonance imaging. Magn Reson Imaging. 2, 1984: 193-204.
60. Wagner, H. N., Jr., and Conti, P. S.
Advances in medical imaging for cancer diagnosis and treatment. Cancer. 67, 1991: 1121-1128.